Optimum relative speed discretization for detection of moving objects in wide band SAR

Abstract: This paper considers Ground Moving Target Indication (GMTI) using Synthetic Aperture Radar (SAR). SAR GMTI requires that Relative Speed between the target and the SAR platform is included in the detection algorithm. A separation between the true Relative Speed and the Relative Speed used in the SAR process will cause unfocused targets, and decrease detectability. Blind hypotheses of Relative Speeds are used in the detection phase of moving targets in SAR. The step size between the hypotheses (or, discretization step) in Relative Speed involves a trade off between the number of hypotheses to test and detectability. A large number of tests will increase detectability but will also increase computation load and vice versa. The relevance of Relative Speed increases as the azimuth integration time gets larger. Long integration time is associated with low signature moving target detection in strong clutter environments, or for SAR GMTI at low frequencies. In this paper we determine the optimum discretization of Normalized Relative Speed (NRS) for moving target detection. The optimum discretization is derived from the moving target impulse response. Use of optimum discretization reduces the computation burden in SAR GMTI and secures the detectability.

1. Introduction

Many interesting papers have been published in the area of SAR GMTI [1-4] in the latest decades. If a moving target is present in a SAR image the target will be displaced and unfocused. This was already described by [5] in the 1970's, for narrow band SAR systems. However, these effects in the SAR image can be used to detect the moving target and to estimate such target properties as position and speed. As soon as the target is detected more computationally demanding techniques can be used to image the target and to get a more accurate estimate of the speed and position. In this paper we discuss the detection phase of SAR GMTI processing.

The complexity of detecting a moving target with a SAR system is illustrated by the complexity of forming a SAR image. The SAR image formation of stationary targets is in principle a two dimensional process in spatial domain. With a moving target present there will be two extra dimensions given by the target motion. SAR is associated with long integration time and image formation of non moving targets demands large computer processing resources. SAR processing of moving targets poses the problem of extreme complexity due to the possibly infinite number of tracks which may be taken by the target during integration time. For the purposes of detection, we therefore assume a track model with constant speed. This

model is used in almost all publications in the field. However there are some publications considering acceleration in SAR GMTI as in [6].

When the moving target is focused we have the highest possibility for detection. Non moving targets are focused according to SAR platform motion. For moving targets it can be shown that all moving targets can be focused in the SAR process by considering the Relative Speed between the target and SAR platform [4]. This means that many moving targets with different ground positions and speeds in the four dimensional space (two ground positions and two speeds) can be focused at the same position in three dimensions, Relative Speed and image position, used in the SAR process. However the three dimensions in the SAR process is a one dimensional sub space of the original four dimensions that will cause an unknown image displacement given by papers [4,7]. The one dimensional sub space is given by an angle described later in this paper. By using the SAR system antenna gain function in combination with SAR focusing, the moving target displacement can be found [8]. However a more common method involves measuring the displacement of the moving target by adding angular measurement capabilities to the system.

The angular dimension is measured by an array antenna at the SAR system. By using Space Time Adaptive Processing (STAP) on the array, detectability in the SAR system increases. Measurements have shown that the Signal to Clutter Noise Ratio (SCNR) increases by 20-30dB even for a short synthetic aperture [7,9]. Normally these short clutter filtered apertures are combined to higher resolution by SAR processing [10-12], which will also increase the SCNR in the detection [7,12]. Due to array elements separations in spatial domain, the radial speed has to be considered at every point along the synthetic aperture. Adding the array produces a four dimensional problem which is given by image position, relative speed and angle or radial speed of the moving target along the synthetic aperture. Assuming linear motion, the image position and Relative Speed are constant while the radial speed changes with a cosine function over the aperture [7]. These four dimensions are measured in [13] using a two channel SAR system.

In SAR moving target detection, a blind search in Relative Speed domain is made for detection. This means that discretization in Relative Speed is valid both for three and four dimensional SAR detection. Detection of low signature targets requires a long integration time. However, in blind integration, the SCNR will basically saturate when the linear motion model fails. The length of time for which the linear model is valid is, in turn, given by the moving target properties, and even more importantly the environment in which the target is moving, in combination with radar system properties such as operational wavelength. The environment influences the target movement and the targets acceleration. The acceleration is for example very different on an off road track compared to a smooth freeway. This means that a low frequency radar system measuring a moving target on a smooth road use a much longer integration time than a high frequency radar system measuring a target on an off road track. By using a priori information (for example, maps) about the illuminated area [14] a

maximum integration time can be found. Adding other priori parameters such as possible targets in that area gives a more accurate integration time. Experimental analyses of different targets have been made in [15], however, the maximum integration time is still an interesting area for research.

Knowing the radar parameters and the maximum integration time this paper aims to derive the optimum discretization step in Relative Speed to test the presence of a moving target. The main difference with regard to other SAR or SAR STAP work is that we in this paper assume longer integration time in the detection phase and thereby require moving hypotheses over many possible Relative Speeds. This procedure involving multiple hypotheses in Relative Speed is mentioned in [12], however, nothing is mentioned about the selection of a discretization in the test. Only [3] derives a discretization step in Relative Speed, using a limitation on the phase error to keep coherence in the SAR integration. As the discretization step increases delectability decreases, causing detection failure in the test. However, as the step decreases the computational load increases. Therefore this article will derive a discretization related to the moving target peak value impulse response in order to keep the computation burden down without losing detectability. In contrast to [16] this paper gives a more general wide band solution and associate discretization step to different types of radar systems.

At higher frequencies, detection with a long integration time is associated with the detection of low signature moving targets in a strong-clutter background. At low frequencies it is associated with the detection of any moving targets which may be concealed, for example, in forested roads [17]. Both areas are of great importance; we have, therefore not made any frequency or bandwidth restrictions in the derivation. This means that we have considered both narrow band and Ultra Wide Band Wide Beam (WB) SAR systems.

This paper is organized as follows: Section II gives an example of a hypothesis test in azimuth integration. This algorithm assumes long integration time thereby making it possible to estimate both along and across track target motion [11]. Section III derives the optimum discretization from the SAR image impulse response. The optimum is found in two ways by an exact solution and by an approximation. In section IV we present results on the discretization step.

2. Hypothesis test in azimuth integration

When a radar system is located on a moving platform, the moving target is often hidden by strong clutter in the Doppler domain [18]. The usual method of separating the moving target from the stationary clutter is to add angular dimension to the radar system by the use of an antenna array. In the two dimensional space of angle and Doppler, the moving target can be detected using STAP [19,20]. By adding SAR capabilities to the system integration time for moving target detection can be increased, and so too can delectability. Long integration time in the detection phase of a moving target will cause non linear

range migration in the detection phase. This section gives an example of a hypothesis test using non linear range integration for the purpose of detection.

Given a Cartesian coordinate system on the ground, the range distance (the Euclidean distance between target and platform) at slow time *t* is given by

$$r_t(t)=\sqrt{\left(\xi_{pl}(t)-\xi_t(t)\right)^2+\left(\eta_{pl}(t)-\eta_t(t)\right)^2+\zeta_{pl}^2(t)} \tag{1}$$

where $\left(\xi_{pl}(t),\eta_{pl}(t),\zeta_{pl}(t)\right)$ is the position of the platform and $\left(\xi_t(t),\eta_t(t),0\right)$ is the position of the moving target at time *t*.

This paper utilises linear motion of the platform $\left(v_{pl}t,0,h\right)$ and the moving target $\left(v_\xi t+\xi_0,v_\eta t+\eta_0,0\right)$, where $\left(v_{pl},0,0\right)$ is the platform speed, $\left(v_\xi,v_\eta,0\right)$ is the moving target speed vector and *h* is the flight height. This means that we do not consider motion in the $\hat{\zeta}$ direction, in this paper. Assuming linear motion the range distance can then be expressed [21,7] as

$$r_t(t)=\sqrt{\gamma_t^2\left(v_{pl}t-x_t\right)^2+y_t^2} \tag{2}$$

with the Normalized Relative Speed (NRS)

$$\gamma_t=\sqrt{\left(v_{pl}-v_\xi\right)^2+v_\eta^2}\Big/v_{pl} \tag{3}$$

and x_t and y_t related to the moving target position in the processed SAR image.

Let $\mathbf{Y}$ be the sampled version of the measurement vector for all antenna channels and at all available measurement times *t*. Under the two hypotheses, with a target present $\mathbf{H_1}$ and with no target present $\mathbf{H_0}$, the likelihood ratio test is given by [22]

$$\Lambda=\frac{P\left(\mathbf{Y}\middle|\mathbf{H_1}\right)}{P\left(\mathbf{Y}\middle|\mathbf{H_0}\right)} \tag{4}$$

The solution of this test in the SAR STAP case can be found in different publications such as [1,10]. In case of time domain fast backprojection SAR processing, the detection algorithm is given by [7]

$$\left|\sum_{m=1}^{M}\frac{1}{R_{cm}^2}\sum_{n=0}^{N-1}e^{jk_n r_m^t}\mathbf{A}_{nm}^H\left(\varphi'_m\right)\mathbf{C}_{nm}^{-1}\tilde{\mathbf{Y}}_{nm}\right|^2=\begin{cases}\geq\lambda & decision\ \ for\ \ \mathbf{H_1}\\ <\lambda & decision\ \ for\ \ \mathbf{H}_0\end{cases} \tag{5}$$

where m is the sub-aperture number, n is the frequency number, $\tilde{\mathbf{Y}}_{nm}$ is sub-aperture beam measurement vector at n and m, $\mathbf{C}_{nm}$ is the covariance matrix at n and m, r_m^t is the range distance to target in sub-aperture beam m, k_n is the wave number at frequency n, R_{cm} is sub-image distance at sub-aperture m ($R_{cm}\approx r_m^t$) and $\mathbf{A}_{nm}\left(\varphi'_m\right)$ is the steering vector at n and m for the moving target, given by

$$\mathbf{A}_{nm}\left(\varphi'_m\right)=\begin{bmatrix}1\\ e^{-jk_n d\left(\cos\varphi_m-\cos\varphi'_m\right)}\\ \vdots\\ e^{-jk_n(L-1)d\left(\cos\varphi_m-\cos\varphi'_m\right)}\end{bmatrix}. \tag{6}$$

The steering vector $\mathbf{A}_{nm}\left(\varphi'_m\right)$ is dependent on d (the distance between the effective antenna phase centers in the array), φ_m is the Doppler angle and φ'_m is the real angle between the flight track and the moving target at sub-aperture m. By a constant d in (6) we have assumed a linear array which is small in comparison to the range distance. In this case, an effective antenna phase center gives a good approximation of the distance change between the channels [23].

If only one antenna channel is used, the steering $\mathbf{A}_{nm}\left(\varphi'_m\right)$ is equal to one. Then the likelihood ratio depends only on three dimensional space: two image positions and Relative Speed. Using only one antenna in the test (5), we will only be able to detect and estimate the Relative Speed, the displacement in position will be unsolved. As seen in (3), all possible solutions in target speed $\left(v_\xi, v_\eta, 0\right)$, connected to one Relative Speed is given by a circle around v_{pl}. In [8] the direction in the circle and the correct position is estimated by using the radar antenna gain function.

With two or more antenna channels there will be a change in phase between the elements in the steering vector $\mathbf{A}_{nm}\left(\varphi'_m\right)$. The separation is caused by radial speed of the moving target and is connected to the Doppler angle φ_m separation from the real angle φ'_m. In this case the likelihood ratio test has to consider the four parameter space given by moving target position

and speed. In (5) these parameters are transformed to image appearance, Relative Speed and displacement in the array. The optimization in the steering vector $\mathbf{A}_{nm}\left(\varphi'_m\right)$ has similarities with other array signal processing steering vector optimization problems and will not be handled in this paper. This paper we will focus only up on the discretization in Relative Speed for detection, which is related to target distance r_m^t in (5) [7,24].

3. Derivation of step size in relative speed

For moving target detection, SAR images are formed at different Relative Speeds, considering range migration given by the hypotheses of NRS γ_p under test. The SAR processing uses the hypotheses of range migration given by

$$r_h\left(t,\gamma_p,x_h,y_h\right)=\sqrt{\gamma_p^2\left(v_{pl}t-x_h\right)^2+y_h^2} \tag{7}$$

The moving target peak value in the SAR image impulse response will be maximized when $\gamma_p=\gamma_t$, $x_h=x_t$ and $y_h=y_t$. Many tests are required in order to ensure secure detection over large areas. Because of the complexity of SAR processing, the number of tested hypotheses should not be more than actually required. This paper relates discretization of NRS to peak value in the impulse response of the moving target. The discretization step will then be optimized to a predefined decrease in the impulse response of the moving target.

If the hypothetic NRS is not equal to the target NRS $\gamma_p\neq\gamma_t$ the target will be unfocused [5]. The shape of the unfocused target is given in [12,25], and can be found from the hyperbolic function

$$r_p\left(t,\gamma_p\right)=\sqrt{\gamma_p^2\left(v_{pl}t-x_p\left(t\right)\right)^2+y_p^2\left(t\right)} \tag{8}$$

where $\left(x_p\left(t\right),y_p\left(t\right)\right)$ gives the trajectory of the unfocused moving target in the SAR image. If $\gamma_p=\gamma_t$ the moving target will be focused and $\left(x_p\left(t\right),y_p\left(t\right)\right)$ is one point and equal to $\left(x_t,y_t\right)$. The relation between $r_p\left(t,\gamma_p\right)$ and $r_t\left(t\right)$ at time *t* is given by range distance and Doppler. The moving target position in the SAR image can be found from

$$r_p\left(t_0,\gamma_p\right)=r_t\left(t_0\right) \tag{9}$$

$$\frac{dr_p\left(t_0,\gamma_p\right)}{dt}=r_p'\left(t_0,\gamma_p\right)=r_t'\left(t_0\right) \tag{10}$$

The SAR algorithm will place the moving target at time t_0 at the image coordinates

$$x_p\left(t_0,\gamma_p\right)=v_{pl}t_0-\frac{\gamma_t^2}{\gamma_p^2}\left(v_pt_0-x_t\right) \tag{11}$$

$$y_p\left(t_0,\gamma_p\right)=\sqrt{\frac{\gamma_t^2}{\gamma_p^2}\left(\gamma_p^2-\gamma_t^2\right)\left(v_{pl}t_0-x_t\right)^2+y_t^2} \tag{12}$$

The trajectory given by these functions relates to three shapes: a hyperbola, a point or an ellipse given by the relation of γ_p and γ_t [12,25].

If $\gamma_p\neq\gamma_t$ there will be a peak value decrease in the moving targets image impulse response compared to the response when $\gamma_p=\gamma_t$. To estimate the decrease connected to NRS we use the time domain global backprojection integral given by [26,27]

$$h\left(\gamma_p,x_h,y_h\right)=\int_{-\infty}^{\infty}g\left(t,r_h\left(t,\gamma_p,x_h,y_h\right)\right)dt \tag{13}$$

where

$$g\left(t,R\right)=\frac{p\left(R-r_t\left(t\right)\right)v_{pl}}{r_t\left(t\right)} \tag{14}$$

and $p(R)$ is the band limited radar pulse after pulse compression as a function of range *R* (fast time). When a chirp pulse is used during transmission, the impulse response is approximately [28]

$$p(R) \approx e^{-j4\pi f_c \frac{R}{c}} \operatorname{sinc}\left(\frac{2\pi BR}{c}\right) \tag{15}$$

where f_c is the center frequency and *B* is the bandwidth of the transmitted wave.

The global backprojection integral in (13) gives the SAR image impulse response. To estimate the decrease in impulse response peak value we compare the processed image under hypotheses $r_h\left(t,\gamma_p,x_h,y_h\right)$ to $r_t\left(t\right)$. The incorrect hypotheses smear the point target into a line given by (11) and (12), and the peak value will be on that line. The ratio between a point on the line t_0 and the focused target is given by

$$h_{ratio}\left(t_0,\gamma_p\right) = \frac{\int_{-\infty}^{\infty} g\left(t, r_p\left(t,t_0,\gamma_p\right)\right)dt}{\int_{-\infty}^{\infty} g\left(t, r_t\left(t\right)\right)dt} \tag{16}$$

where

$$r_p\left(t,t_0,\gamma_p\right) = \sqrt{\gamma_p^2\left(v_{pl}t - x_p\left(t_0\right)\right)^2 + y_p^2\left(t_0\right)} \tag{17}$$

In reality there is a limit for the linear motion model. The limit depends on oscillation and rotation of the moving target in connection with the radar system parameters, discussed in the introduction. The integration time has to be selected according to the priori information. We assume that the linear model is valid during time $t_i = t_2 - t_1$ (where $t_1 < t_0 < t_2$) and that the SAR peak value impulse response ratio is given at $t_0 = t_0^m$. By using (14), (15) and (16) the ratio is

$$h_{ratio}\left(t_0^m,\gamma_p\right)=\frac{\int_{t_1}^{t_2}\frac{e^{-j4\pi f_c\frac{\Delta r\left(t,t_0^m,\gamma_p\right)}{c}}\operatorname{sinc}\left(\frac{2\pi B\Delta r\left(t,t_0^m,\gamma_p\right)}{c}\right)}{r_t\left(t\right)}dt}{\int_{t_1}^{t_2}\frac{1}{r_t\left(t\right)}dt} \tag{18}$$

where

$$\Delta r\left(t,t_0,\gamma_p\right)=r_p\left(t,t_0,\gamma_p\right)-r_t\left(t\right). \tag{19}$$

is the distance error caused by incorrect NRS. The reduction in impulse response peak value is given by $\left|h_{ratio}\left(t_0^m,\gamma_p\right)\right|$. Assume that the maximum acceptable reduction in $\left|h_{ratio}\left(t_0^m,\gamma_p\right)\right|$ caused by discretization is given by h_{limit}. Then a step δ in NRS between true NRS $\gamma_p=\gamma_t$ to the closest discretization in NRS causes a reduction $\left|h_{\text{ratio}}\left(t_0^m,\gamma_t+\delta\right)\right|\geq h_{\text{limit}}$. To secure detection δ should be set to maximum step which is $\delta=\pm\Delta\gamma_p/2$, where $\Delta\gamma_p$ is the discretization step in NRS and $\left|h_{\text{ratio}}\left(t_0^m,\gamma_t\pm\Delta\gamma_p/2\right)\right|=h_{\text{limit}}$. We will now look at the solution to this problem for short aperture and then compare to the general solution.

3.1 Short aperture L<<y_t

Often the aperture defined by the integration time is much smaller than the platform to target distance. The ratio is then approximately given by

$$h_{ratio}\left(t_0,\gamma_p\right)\approx\frac{1}{t_i}\int_{t_1}^{t_2}e^{-j4\pi f_c\frac{\Delta r\left(t,t_0,\gamma_p\right)}{c}}\operatorname{sinc}\left(\frac{2\pi B\Delta r\left(t,t_0,\gamma_p\right)}{c}\right)dt \tag{20}$$

The ratio $h_{ratio}\left(t_0,\gamma_p\right)$ decreases when integration time t_i and therefore $\Delta r\left(t,t_0\right)$ increases. Even for a narrow band SAR system, the ratio decrease when $\Delta r\left(t,t_0,\gamma_p\right)$ has approximately the same size as the radar system wave length $\lambda_c=c/f_c$. As a

consequence, $\Delta r\left(t,t_0,\gamma_p\right)$ is very small in comparison to the range distance. If the aperture $L=v_{pl}t_i$ is also considerably smaller than the range distance, the error can be approximated by a Taylor extension around t_0

$$\Delta r\left(t,t_0,\gamma_p\right)=\Delta r\left(t_0,t_0,\gamma_p\right)+\Delta r'\left(t_0,t_0,\gamma_p\right)\left(t-t_0\right)+\frac{\Delta r''\left(t_0,t_0,\gamma_p\right)\left(t-t_0\right)^2}{2}+R_3\left(t\right) \tag{21}$$

where the first order derivative is given by

$$\Delta r'\left(t,t_0,\gamma_p\right)=\frac{d\Delta r\left(t,t_0,\gamma_p\right)}{dt}=v_{pl}\left(\frac{\gamma_p\tilde{x}_p\left(t,t_0,\gamma_p\right)}{\sqrt{\tilde{x}_p^2\left(t,t_0,\gamma_p\right)+y_p^2\left(t_0,\gamma_p\right)}}-\frac{\gamma_t\tilde{x}_t\left(t\right)}{\sqrt{\tilde{x}_t^2\left(t\right)+y_t^2}}\right) \tag{22}$$

using

$$\begin{aligned}\tilde{x}_p\left(t_0,\gamma_p\right)&=\gamma_p\left(v_{pl}t-x_p\left(t_0\right)\right)\\ \tilde{x}_t\left(t\right)&=\gamma_t\left(v_{pl}t-x_t\right)\end{aligned} \tag{23}$$

and the second order derivative

$$\Delta r''\left(t,t_0,\gamma_p\right)=v_{pl}^2\left(\frac{\gamma_p^2y_p^2\left(t_0,\gamma_p\right)}{\left(\tilde{x}_p^2\left(t,t_0,\gamma_p\right)+y_p^2\left(t_0,\gamma_p\right)\right)^{3/2}}-\frac{\gamma_t^2y_t^2}{\left(\tilde{x}_t^2\left(t\right)+y_t^2\right)^{3/2}}\right) \tag{24}$$

Because $x_p\left(t_0\right)$ and $y_p\left(t_0\right)$ is found from range distance $r_p\left(t,t_0,\gamma_p\right)=r_t\left(t_0\right)$ and the first order derivative $r_p'\left(t,t_0,\gamma_p\right)=r_t'\left(t_0\right)$, the second order derivative is

$$\Delta r''\left(t_0,t_0,\gamma_p\right)\approx v_{pl}^2\frac{\left(\gamma_p^2-\gamma_t^2\right)}{r_t\left(t_0\right)} \tag{25}$$

and the error distance $\Delta r\left(t,t_0,\gamma_p\right)$ is given by

$$\Delta r\left(t,t_0,\gamma_p\right)=\frac{\Delta r''\left(t_0,t_0,\gamma_p\right)\left(t-t_0\right)^2}{2}+R_3\left(t\right)\approx v_{pl}^2\frac{\left(\gamma_p^2-\gamma_t^2\right)}{r_t\left(t_0\right)}\frac{\left(t-t_0\right)^2}{2} \tag{26}$$

For short apertures, a good approximation of t_0^m is $t_0^m=t_i/2+t_1$. Using this symmetry in time and (26) the integral in (20) (when $\gamma_p>\gamma_t$) can be approximated to

$$h_{ratio}\left(Q,q\right)\approx\frac{1}{2Q}\int_{-Q}^{Q}e^{-jp^2}\,\mathrm{sinc}\left(qp^2\right)dp \tag{27}$$

where $Q=\chi\sqrt{\pi\left(\gamma_p^2-\gamma_t^2\right)/2}$ and the radar dependent parameters $q=B/f_c$ and $\chi=L/\sqrt{\lambda_c r\left(t_0^m\right)}$. When $\gamma_p<\gamma_t$ the integral will be a complex conjugate to (27) (symmetric around γ_t) with $Q=\chi\sqrt{\pi\left(\gamma_t^2-\gamma_p^2\right)/2}$. We therefore use

$$Q=\chi\sqrt{\frac{\pi}{2}\left|\gamma_p^2-\gamma_t^2\right|} \tag{28}$$

for all NRS. Because the peak value is an absolute value, the complex argument does not matter and (27) can be used for all NRS using (28). The absolute value of the integral in (27) is shown in Figure 1. Knowing the relative band width *q* and the maximum loss h_{limit} the Q can be found from (27). From *Q* the optimum discretization step is found to be

$$\Delta\gamma_p=2\left(\sqrt{\gamma_t^2+\frac{2Q^2}{\pi\chi^2}}-\gamma_t\right) \tag{29}$$

and when the discretization step is small

$$\Delta\gamma_p\approx\frac{2Q^2}{\pi\gamma_t\chi^2} \tag{30}$$

3.2 Long aperture

In the case of a long integration time, the approximation given in (20) and (26) is not valid. However, this section will show that the approximate solution for short integration time can be used for apertures up to $L=y_t$ with a discretization error less then 10%.

In (20) the decrease in amplitude due to the distance from the target is neglected in comparison to (18). For long apertures the windowing effect of range will decrease the influence of time close to t_1 or t_2 in the integration of (18), where $\Delta r\left(t,t_0,\gamma_p\right)$ takes its maximum value. For long apertures there will also be a windowing effect given by the antenna gain not considered in this work. This means that the phase error has a larger influence in (20) than in (18), and that (20) gives a smaller discretization step than (18). The windowing effect can be seen as a smaller effective aperture. In Figure 2 (20) is compared with (18), and as mentioned, (20) gives a discretization step a little bit smaller than (18).

The Taylor approximation in (26) is not valid for large apertures, and we should therefore rewrite the exact solution in (19) to a form similar to (26). Equation (19) can be rewritten to

$$\Delta r\left(t,t_0,\gamma_p\right)=r_p\left(t,t_0,\gamma_p\right)-r_t\left(t\right)=\frac{r_p{}^2\left(t,t_0,\gamma_p\right)-r_t^2\left(t\right)}{r_p\left(t,t_0,\gamma_p\right)+r_t\left(t\right)} \tag{31}$$

and using (11) and (12)

$$\Delta r\left(t,t_0,\gamma_p\right)=\frac{\left(\gamma_p{}^2-\gamma_t^2\right)v_{pl}{}^2\left(t-t_0\right)^2}{r_p\left(t,t_0,\gamma_p\right)+r_t\left(t\right)} \tag{32}$$

In comparison to the Taylor approximation in (26), the above equation depends on the quadratic term and on the range distance. It is also seen that the two equations (26) and (32) give the same value for small apertures.

Let us now compare the exact solution with the approximate in the integration of (20). Dividing the exact solution by the approximate we get

$$\frac{2r_t(t_0)}{r_p(t,t_0,\gamma_p)+r_t(t)} \approx \frac{r_t(t_0)}{r_t(t)} \tag{33}$$

Where $r_p(t,t_0,\gamma_p)+r_t(t) \approx 2r_t(t)$ is a very accurate approximation because the separation between $r_p(t,t_0,\gamma_p)$ and $r_t(t)$ is only a number of wavelengths λ_c which is very small compared with the range distance. We see that the introduced error using (26) in the integration of (20) only depends on range distance. This means that even when L is in the size of y_t the approximate solution gives a good estimate of the discretization step.

For large apertures, the minimum distance $r_t(t_0^m)=y_t$ is the natural choice for t_0^m. According to the ratio presented in (33) the exact solution is always smaller than the approximate solution. Therefore, the approximate derived discretization step is a little smaller than that derived by the exact solution. The ratio in (33) also shows that the difference between the exact and the approximate solutions only depends on the product $\gamma_t L/y_t$. Figure 2 compares the approximate solution using (26) and (20) (or Equation (29)) with the exact solution in (18) using (19). Figure 2 can then be used to compensate, bringing the value of the approximate solution closer to that of the real solution. We also find that, for large apertures with $\gamma_t L \le y_t$, the approximate solution gives a discretization step error less then 10%.

4. Results

The optimum relative speed discretization is derived in this paper considering the moving target impulse response. In a situation when the processed relative speed differs from the moving target relative speed there will be a loss in the target peak value impulse response. The loss may cause a detection failure in the likelihood ratio test (5). To estimate the loss we have defined the target peak value impulse response ratio h_{ratio}. The ratio gives the loss caused by incorrect relative speed, and is given by (18). In Figure 3 calculations of (18) are presented for a radar system with minimum distance of 10000 meter, with two different frequencies and with three different synthetic apertures. As expected, the ratio gets more sensitive to relative speed as the frequency or synthetic aperture increases. At 500MHz and with a synthetic aperture L=100 meter a change in relative speed by 0.1 cause a very small change in the target peak value, however, with the same aperture but at 10GHz a change in relative speed with only 0.02 will cause a loss close to 2dB, as illustrated in Figure 3. Given a maximum acceptable decrease in the impulse response peak value ratio h_{limit}, the optimum discretization can be found from (18). In Table 1 the optimum relative speed is calculated using (18) for three different radar systems. In the table the speed product

$\Delta\gamma_p v_{pl}$ in the along track direction is given to illustrate the sensitivity to relative speed. As seen in Figure 2, the difference between (18) and (29) is less then 10% for $\gamma_t L \le y_t$. Because (29) gives a smaller discretization step, it is associated with smaller peak value decrease than (18). The approximate quadratic solution is more illustrative in a mathematical point; we will use the approximation in this section. The result can easily be adjusted to the exact solution, using Figure 2.

Assume that a target performs linear motion during time t_i which sets the maximum SAR detection aperture to *L*. The optimum discretization is then illustrated by Figure 4. Increasing the synthetic aperture by two will decrease the NRS discretization step by four. The decrease in the discretization step will increase the computation load up to the same magnitude. As illustrated by Figure 4 the bandwidth has an impact on the discretization step in NRS. Increase in bandwidth results in a smaller discretization step in NRS, if h_{limit} is kept at a constant level. In Figure 5 this is illustrated with three different h_{limit} curves: -3dB, -0.5dB and -0.1. The step is normalized to the maximum discretization step $\Delta\gamma_p^{\max} = \lim_{B\to 0}\Delta\gamma_p$, in order to plot all three cases in the same figure.

In most cases, *L* is small in comparison to the minimum range y_t. In this case the optimum discretization will change over the aperture as a function of direction φ. In Figure 5 this is illustrated where γ_p is normalized with $\Delta\gamma_p^{\min} = \lim_{\varphi\to 0}\Delta\gamma_p$.

5. Discussion

This paper gives a optimum discretization step in NRS for the detection of moving targets in SAR systems. The levels are found considering integration time and the radar system parameters. In the process we assume the detection as a one stage SAR process using global backprojection. However, time domain processing is not critical and the results can be applied to any SAR algorithm. In all algorithms a synthetic aperture length is used, and therefore an optimum discretization can be found.

The detection methods for moving targets are often given by two stages in the algorithm [7,10]. As mentioned in the introduction, the detection of a moving target may be seen as a three dimensional problem. However, if an array antenna is added the detectability increases and the moving target displacement can be measured. An example of such a method is given in Section II. After the first stage in the SAR process the strong clutter return is cancelled using space time processing. In the second stage the resolution of the target is increased. In the first stage, the aperture is short and the discretization step large and probably only one or two NRS levels are needed in the hypotheses test. The number of levels required and the target impulse response peak value reduction can be found using the optimum discretization derived in this paper. In the second stage a larger aperture is formed and results in an increase in number of discretization levels required. The total peak value reduction can be found using the reduction in the two stages.

In multistage backprojection techniques such as [29,30] there are many stages involved in moving target SAR processing. Processing speed can be increased using the optimized discretization in every stage. The total peak value reduction is calculated by using the value of the loss in each stage.

6. Conclusions

This paper has examined the discretization in Relative Speed for moving target detection in SAR systems. We have derived the optimum discretization in the Normalized Relative Speed (NRS) as a function of the peak value decrease in the moving target SAR image impulse response. The peak value decrease is determined using the global back projection integral.

It is found that the quadratic phase error approximation in the derivation of a discretization step in NRS is a good approximation as long as the integration aperture is considerably smaller than the range distance. It is also found that the approximation can be used for aperture sizes up to the minimum range distance, with an error less than 10%.

This paper also examined the discretization step dependence on relative bandwidth. It is found in one example that a narrow bandwidth system has a discretization step 33% larger than the broad bandwidth system. Therefore the processing speed in a narrow bandwidth system may be faster than that of a broad band system. It is also found that, at large squint angles, the discretization step can be up to 100% bigger than at broad side. Using this larger step in the detection phase saves computation load.

7. Acknowledgement

The author would like to thank the Swedish Knowledge Foundation and the industry partners Saab Bofors Dynamics, Ericsson Microwave System and Saab Space for the support that makes this research project possible.

8. References

[1] Ender, J.H.G.: ‘Space-time processing for multichannel synthetic aperture radar’, Electronics & Communication Engineering Journal, 1999, **11**, (1), pp. 29-38

[2] Barbarossa, S.: ‘Detection and imaging of moving objects with synthetic aperture, Part 1: Optimum detection and parameter estimation theory’, IEE Proceedings-F, 1992, **139**, (1), pp 79-88

[3] Hellsten, H., and Ulander, L.M.H.: ‘Airborne array aperture UWB UHF radar-motivation and system considerations’, IEEE Aerospace and Electronic Systems Magazine, 2000, **15**, (5), pp 35-45

[4] Soumekh, M.,: 'Moving Target Detection in Foliage Using Along Track Monopulse Synthetic Aperture Radar Imaging', IEEE Transactions on Image Processing, 1997, **6**, (8), pp. 1148-1162

[5] Raney, R. K.: 'Synthetic Aperture Imaging Radar and Moving Targets', IEEE Transactions on Aerospace and Electronic Systems, 1971, **7**, (3), pp. 499-505

[6] Sharma, J.J., Gierull, C.H., Collins, M.J.: 'The Influence of Target Acceleration on Velocity Estimation in Dual-Channel SAR-GMTI', IEEE Transactions on Geoscience and Remote Sensing, 2006, **44**, (1), pp. 134-147

[7] Pettersson, M.I., 'Detection of moving targets in wideband SAR', IEEE Transactions on Aerospace and Electronic systems, 2004, **40**, (3), pp. 780-796

[8] Dias, J.M.B., Marques, P.A.C.: 'Multiple Moving Target Detection and Trajectory Estimation Using a Single SAR Sensor', IEEE Transactions on Aerospace and Electronic systems, 2003, **39**, (2) , pp. 604-624

[9] Farina, A., Lombardo P. and Pirri, M.: 'Nonlinear STAP processing', IEE Electronics & communication engineering journal, 1999, **11**, pp. 41-48

[10] Farina, A. and Lombardo, P.: ' Space time techniques for SAR', in Klemm, R. (Ed.): Applications of Space-Time Adaptive Processing, (IEE Press, IEE Radar, Sonar and Navigation series, 2004), pp. 73-120

[11] Perry, R.P., DiPietro, R.C., Fante, R.L.: 'SAR imaging of moving targets', IEEE Transactions on Aerospace and Electronic Systems, 1999, **35**, (1), pp. 188-200

[12] Jao, J.K.: 'Theory of synthetic aperture radar imaging of a moving target', Transactions on Geoscience and Remote Sensing, IEEE, 2001, **39**, (9), pp. 1984-1992

[13] Gierull, C.H.: ' Ground moving target parameter estimation for two-channel SAR', IEE Proceedings, Radar-Sonar Navigation, 2006, **153**, (3), pp. 224-233

[14] Adve, R.S., Wicks, M.C., Hale, T.B., Antonik, P.: 'Ground moving target indication using knowledge based space time adaptive processing', IEEE International Radar Conference 2000, USA, 2000, pp.735-740

[15] Eaton, C. J., and Coe, D. J.: 'Motion of ground moving targets and implications for aided recognition', IEE Radar 2002, Edinburgh, UK, 2002 pp. 370-374

[16] Pettersson, M.: 'Relative speed step size in SAR processing for moving target detection', Proceedings of 2006 CIE International conference on radar, Shanghai, China, Oct. 2006, pp. 991-995

[17] Ulander, L.M.H., Frölind, P.O., Gustavsson, A., Hellsten, H., and Larsson, B.: 'Detection of Concealed Ground Targets in CARABAS SAR Images using Change Detection', Proceedings of SPIE Conference on Algorithms for Aperture Radar Imagery VI, 3721, Orlando, USA, 1999, pp. 243-252

[18] Skolnik, M. I.: 'Radar Handbook', (McGraw-Hill, New-York, 1970)

[19] Ward, J.: ‘Space -Time Processing for Airborne Radar’: Lincoln lab, Massachusetts institute of technology, Technical Report No. 1015, 1994

[20] Klemm, R.: ‘Space- Time Adaptive Processing; principles and applications’: (Institution of Electrical Engineers, 1998)

[21] Hellsten, H. and Ulander, L.M.H.: ‘Airborne Array Aperture UWB UHF-Motivation and System Consideration’, Proceedings of the 1999 IEEE Radar Conference –Radar to the next millenium, Waltham, USA, 1999, pp. 47-53

[22] Trees, H.L.V.: ‘Detection Estimation and Modulation Theory, Part I’, (John Wiley & Sons, New York, 1968)

[23] Pettersson, M.I.: ‘Extraction of moving ground targets by a bistatic ultra-wideband and -widebeam SAR system’, IEE Proc. Radar, Sonar and Navigation, 2001, **148**, (1), pp. 35-40

[24] Pettersson, M.I.: ‘Focusing of Moving Targets in an Ultra-wide band SAR GMTI System’, Proceedings of EUSAR 2000, 3rd Europian Conference on Synthetic Aperture Radar, Germany, 2000, pp. 837-840

[25] Pettersson, M.I., Zetterberg, V., Claesson, I.: ‘Detection and imaging of moving targets in wide band SAS using fast time back projection combined with STAP’, Proceedings of Oceans 2005 MTS/IEEE Conference “One Ocean”., USA. 2005

[26] Fawcett, J.A.: ‘Inversion of N-dimensional spherical averages’, SIAM J. of Appl. Math., 1985, **45**, (2), pp 336-341

[27] Andersson, L.E.: ‘On Determination of a Function from Spherical Averages’, SIAM J. of Appl. Math., 1998, **19**, (1), pp 214-341

[28] Cook, C.E. and Bernfeld, M.: ‘Radar Signals – an Introduction to Theory and Application’, (Artech House, Norwood, 1993)

[29] McCorkle, J., and Rofheart, M.: ‘An order N2log(N) backprojector algorithm for focusing wide-angle wide-bandwidth arbitary-motion synthetic aperture radar’, Proceedings of SPIE Conference on Radar Sensor Technology, Vol. 2747, Orlando, 1996, pp. 25-36

[30] Ulander, L.M.H., Hellsten, H., Stenström, G.: ‘Synthetic-Aperture Radar Processing using Fast Factorised Back-Projection’, IEEE Transactions on Aerospace and Electronic Systems, 2003, **39**, (3), pp.760-776

Table 1: Optimum relative speed discretization for three different radar systems: two air based systems and one satellite based system. The air based systems operates with a minimum range of 1000 meter or 10000 meter. The satellite based system has approximately the TerraSAR-X system parameters. The table is calculated assuming a target moving in the along track direction, $v_{\xi} = -10\,\mathrm{m/s}$.

Aperture		**Low frequency system** $f_c = 500\,\mathrm{MHz}$ $B = f_c$ $v_{pl} = 100\,\mathrm{m/s}$ $\gamma_t = 1.1$		**Microwave system** $f_c = 10\,\mathrm{GHz}$ $B = 1\,\mathrm{GHz}$ $v_{pl} = 100\,\mathrm{m/s}$ $\gamma_t = 1.1$		**Satellite based system** $f_c = 9.65\,\mathrm{GHz}$ $B = 150\mathrm{MHz}$ $v_{pl} = 7600\,\mathrm{m/s}$ $\gamma_t \approx 1.0013$
		$y_t = 1000\,\mathrm{m}$	$y_t = 10000\,\mathrm{m}$	$y_t = 1000\,\mathrm{m}$	$y_t = 10000\,\mathrm{m}$	$y_t = 760000\mathrm{m}$
$L = 100\,\mathrm{m}$	$\Delta\gamma_p$	$8.90 \cdot 10^{-2}$	$8.20 \cdot 10^{-1}$	$4.73 \cdot 10^{-3}$	$5.09 \cdot 10^{-2}$	
	$\Delta\gamma_p v_{pl}$	$8.9\ m/s$	$82\ m/s$	$0.473\ m/s$	$5.09\ m/s$	
$L = 500\,\mathrm{m}$	$\Delta\gamma_p$	$3.75 \cdot 10^{-3}$	$3.91 \cdot 10^{-2}$	$1.96 \cdot 10^{-4}$	$2.06 \cdot 10^{-3}$	
	$\Delta\gamma_p v_{pl}$	$0.375\ m/s$	$3.91\ m/s$	$1.96 \cdot 10^{-2}\ m/s$	$0.206\ m/s$	
$L = 1000\,\mathrm{m}$	$\Delta\gamma_p$	$1.03 \cdot 10^{-3}$	$9.86 \cdot 10^{-3}$	$5.36 \cdot 10^{-5}$	$5.16 \cdot 10^{-4}$	$3.58 \cdot 10^{-2}$
	$\Delta\gamma_p v_{pl}$	$0.103\ m/s$	$0.986\ m/s$	$5.36 \cdot 10^{-3}\ m/s$	$0.0516\ m/s$	$271\ m/s$
$L = 4400\,\mathrm{m}$	$\Delta\gamma_p$					$1.87 \cdot 10^{-6}$
	$\Delta\gamma_p v_{pl}$					$14.2\ m/s$

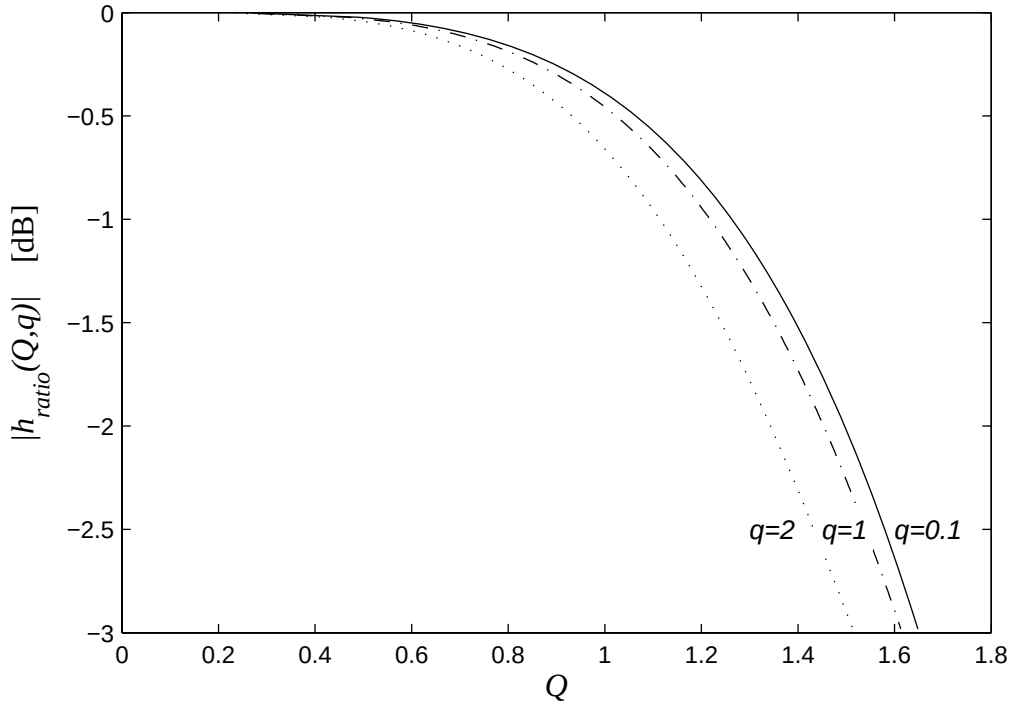

Figure 1. The impulse response ratio $\left|h_{ratio}\left(Q,q\right)\right|$ in (27) given as a function of Q. The three curves correspond to $q=0.1$, $q=1$ and $q=2$.

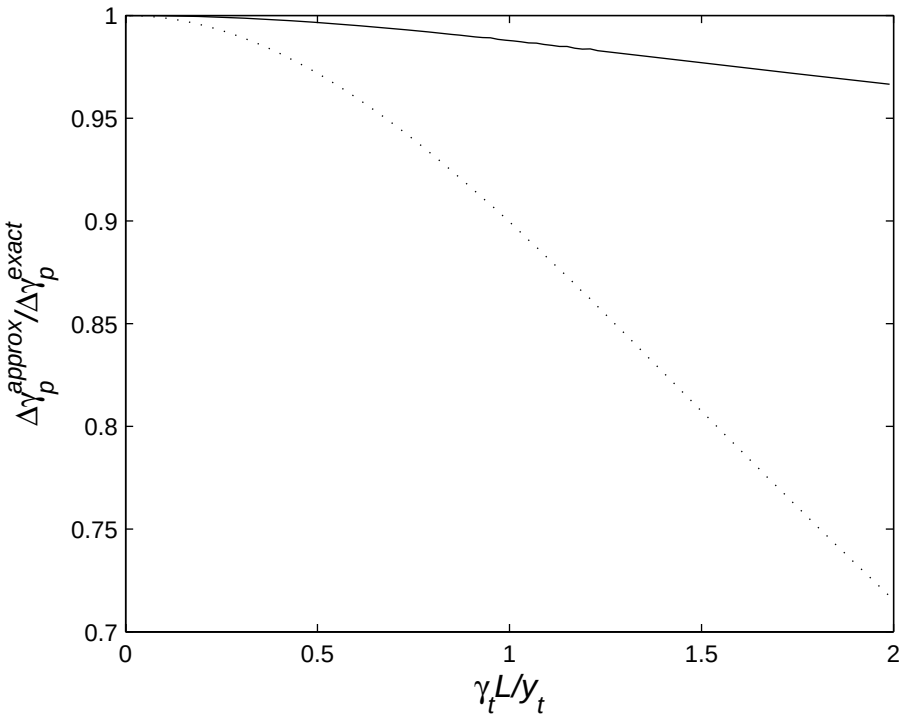

Figure 2. The influence of approximations in Equations (20) and (29) of the discretization step as a function of the product $\gamma_t L/y_t$. The solid line represents the ratio between the approximative Equation (20) and the exact Equation (18), using the exact range (19) in both cases. The dotted line refers to the approximate solution (29) in comparison to the exact solution (18) with exact range (19).

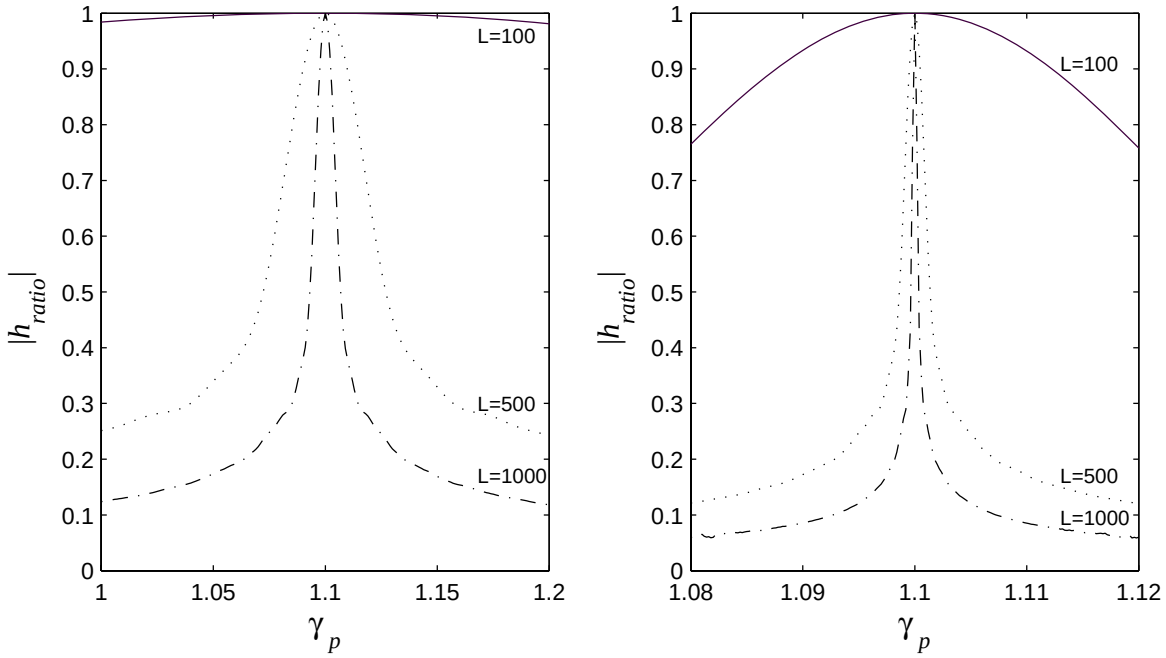

Figure 3. The moving target peak value ratio (18) calculated for three different synthetic apertures $L = 100$, $L = 500$ and $L = 1000$ at a minimum distance of $y_t = 10\,\text{km}$. To the left the ratio is calculated for a center frequency and bandwidth of $B = f_c = 500\,\text{MHz}$ and to the right $B = f_c = 10\,\text{GHz}$. The platform speed is $v_{pl} = 100\,\text{m/s}$ and the target speed is $v_{\xi} = -10\,\text{m/s}$ in both cases.

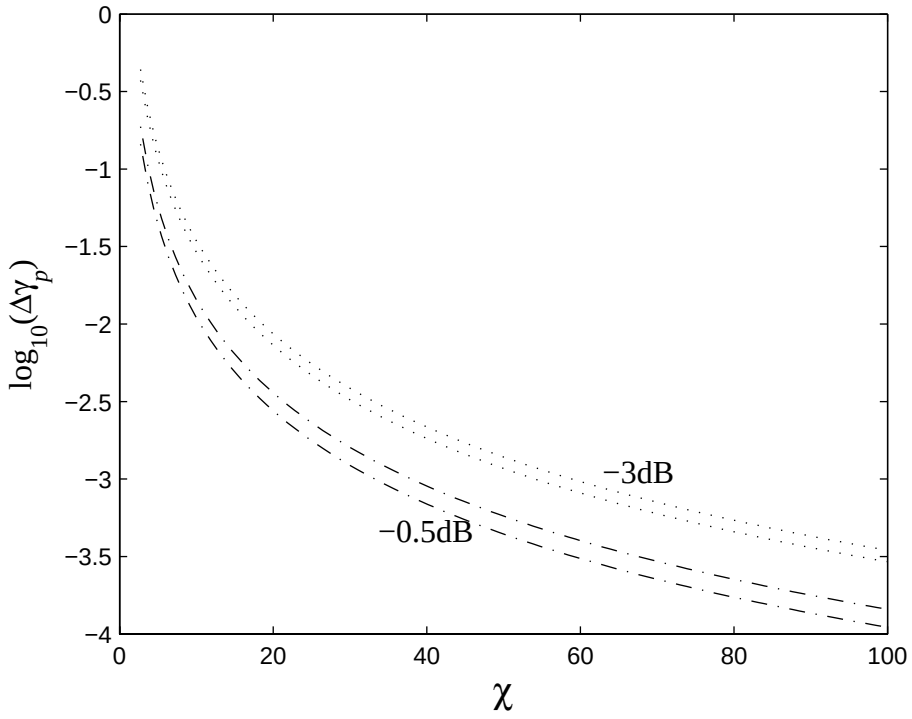

Figure 4. The optimum step size as a function of the radar dependent parameter χ given in (27). Four lines are given with different h_{limit} and relative bandwidth. The two dotted lines with the biggest step value are associated with impulse response ratio $h_{\text{limit}} = -3dB$ and the other two lines with $h_{\text{limit}} = -0.5dB$. In each group the biggest step is associated with narrow bandwidth *q=0.01* and the smallest step with broad bandwidth *q=2*.

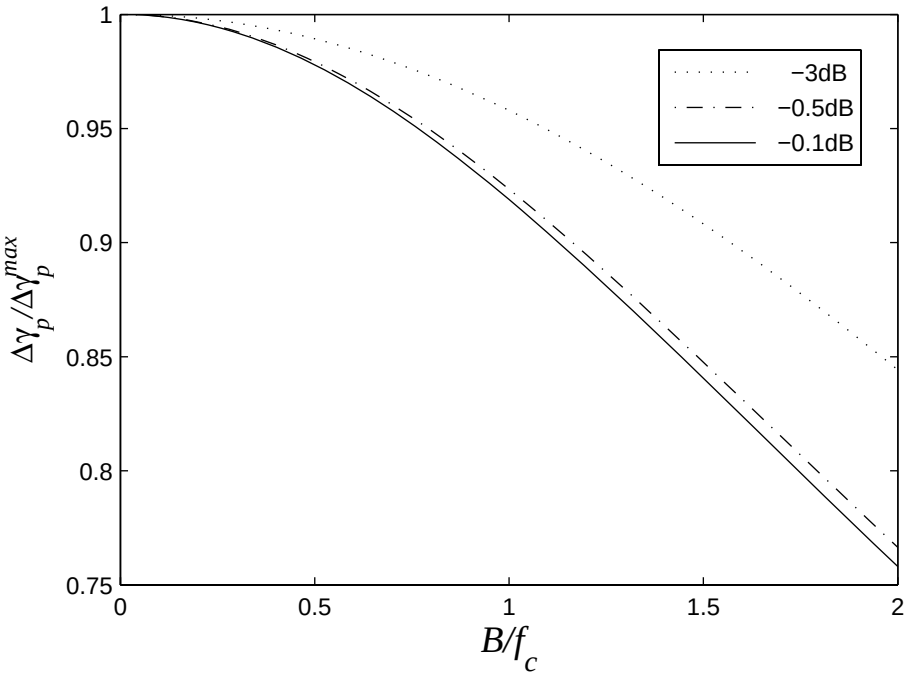

Figure 5. The normalized discretization step as a function of relative bandwidth. The three curves correspond to h_{limit} is equal to -0.1dB, -0.5dB and -3dB, respectively. In the calculation χ is equal to 10 and the $\Delta\gamma_p^{\max} = \lim_{B\to 0}\Delta\gamma_p$.

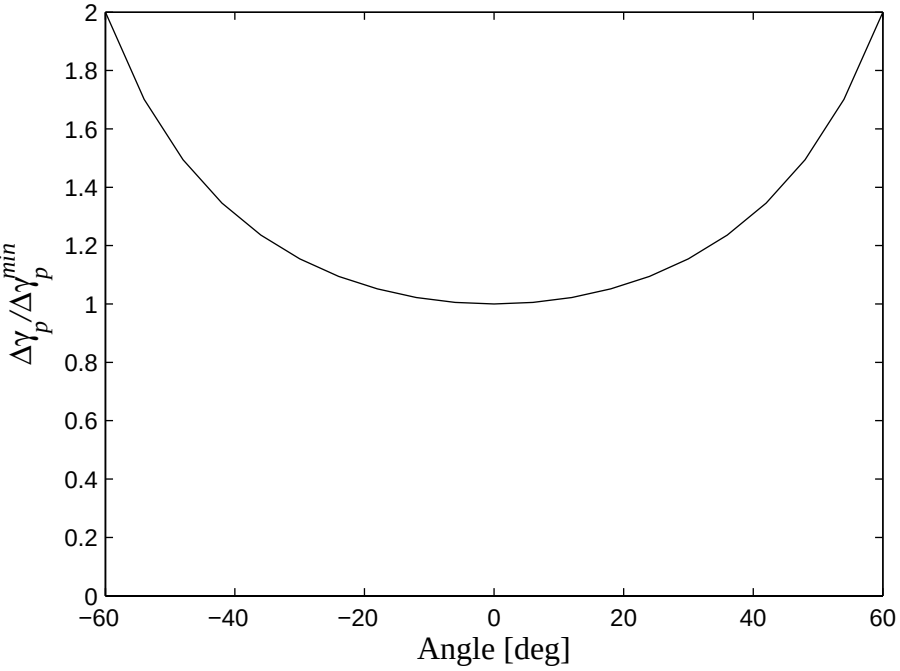

Figure 6. The normalized discretization step as a function of direction angle. The curve assumes a relatively small L and the step is normalised with the step at broad side $\Delta\gamma_p^{\min} = \lim_{\varphi\to 0}\Delta\gamma_p$.